complexes of limited stability employing exodentate sulfur donors is in marked contrast to the remarkable stability of complexes of 9S3 for which the sulfur atoms are preorganized in an endodentate arrangement prior to coordination.[1,2]

Since the conformational preferences of the free crown thioether ligands can profoundly influence their coordination chemistry, we have undertaken a careful study of the molecular mechanics and solid-state structures of TTMB and TTOB.

For TTMB, the X-ray structure and the structure calculated from molecular mechanics minimization indicate that there is an excellent match of the spatial requirements of the *m*-xylyl and the $-SCH_2CH_2SCH_2CH_2S-$ bracket fragments. The sulfur to sulfur distance (6.74 Å, MMX; 6.84 Å, X-ray), which could be described as the "bite" of the bracket, matches exactly the corresponding spacing between benzylic carbon atoms. The results are that neither of the fragments shows appreciable distortion (S-C-C-S of approximately 180°) as a result of their fusion to form the intact TTMB molecule and the three sulfur atoms are exodentate to the ring.

Both X-ray analysis and molecular mechanics calculations show that the basic conformation of TTOB is the same as for TTMB with the three sulfur atoms exodentate to the ring. However, the experimental (166.7 (4)/158.5 (4)°, X-ray) and calculated (174.2/154.4°, MMX) S-C-C-S torsional angles associated with the bracket portion and the smaller S1···S3 spacing (5.76 Å, MMX; 5.80 Å, X-ray) indicate that the $-SCH_2CH_2SCH_2CH_2S-$ bracket must be distorted significantly to adapt to the smaller spatial requirements of the *o*-xylyl fragment.

In order to determine whether TTMB and TTOB could adopt a ligand conformation suitable for facial coordination to a metal, molecular mechanics calculations were performed on the all endodentate conformations of these macrocycles. These results and those obtained similarly for 9S3 indicated that only TTOB could adopt an endodentate geometry that would be suitable for facial coordination. For TTOB, the S1···S2 and S2···S3 distances (3.31 Å) are very close to those obtained for 9S3 (3.34 Å) and the S1···S3 distance across the *o*-xylyl fragment is only slightly longer (3.64 Å). However for TTMB, the S1···S2 and S2···S3 distances are longer (3.53 Å) and the S1···S3 distance (5.94 Å) is clearly incompatible with the proposed geometry.

The predictive value of the molecular mechanics calculations was tested by attempting to coordinate TTOB and TTMB, as a tridentate ligand, to the organometallic fragment *fac*-$Mo(CO)_3$. Only the complex *fac*-$Mo(CO)_3$(TTOB) could be obtained. By comparison of the molecular mechanics calculated geometry for the all-endodentate conformation of TTOB with the conformation of TTOB found in the X-ray structure of $Mo(CO)_3$(TTOB)·DMSO, some conclusions as to the reliability and usefulness of these calculations can be attained. In the complex *fac*-$Mo(CO)_3$(TTOB), the ligand TTOB adopts the all-endodentate conformation and coordinates to the metal by employing all three S donor atoms. The S1···S2 and S2···S3 distances are 3.31 and 3.33 Å, and the S1···S3 distance is 3.80 Å. These are very close to those predicted by molecular mechanics for the all-endodentate conformation in the absence of the metal atom. At least in the simple case of TTOB and TTMB, it appears that molecular mechanics calculations may be useful in the design of crown thioether ligands.

A comparison of the structure of *fac*-$Mo(CO)_3$(TTOB) to those of *fac*-$Mo(CO)_3$(9S3),[18] *fac*-$Mo(CO)_3$(10S3),[9] and *fac*-$Mo(CO)_3$(TTN)[32] shows that TTOB binds in essentially the same geometry as the other crown thioether ligands. Table VIII shows a comparison of various structural parameters within the coordination sphere of these complexes. The major differences are due to the seven-membered chelate ring containing the *o*-xylyl ring. For example, the S1-Mo-S3 angle within the larger chelate is 96.5 (1)° as compared to 82.8 (2)° found for the five-membered chelate in $Mo(CO)_3$(9S3). Although some of these differences are significant, the stability of the complex *fac*-$Mo(CO)_3$(TTOB) seems to be quite comparable to that of *fac*-$Mo(CO)_3$(9S3) and *fac*-$Mo(CO)_3$(10S3). Further studies in our laboratories are under way to determine whether TTOB can function as a ligand for other transition metals. If this comparison to 9S3 can be extended to other metals and complex geometries, this may result in the observation of some unique reaction and redox chemistry.

Acknowledgment. We thank the Natural Sciences and Engineering Research Council of Canada and the donors of the Petroleum Research Fund, administered by the American Chemical Society, for financial support of this research. The Chemistry Department of the University of Manitoba is gratefully acknowledged for the use of their NMR facilities and as the home department of graduate student B.d.G.

Supplementary Material Available: Listings of crystallographic data collection parameters (Table S-I), atomic positional parameters (Tables S-II, S-VI, and S-X), non-essential bond distances and angles (Tables S-III, S-VII, and S-XI), thermal parameters (Tables S-IV, S-VIII, and S-XII), and hydrogen atom parameters (Tables S-V, S-IX, and S-XIII) (9 pages); listings of observed and calculated structure factors (Tables S-XIV-S-XVI) (27 pages). Ordering information is given on any current masthead page.

Contribution from the Department of Chemistry,
York University, North York, Ontario, Canada M3J 1P3

Silver(II) Tetraneopentoxyphthalocyanine and Its Redox Chemistry

Guoyi Fu, Yansong Fu, K. Jayaraj, and A. B. P. Lever*

Received February 27, 1990

The synthesis and characterization of the title complex is described. This new silver(II) phthalocyanine is soluble in most organic solvents, rendering it suitable for extended study. The complex can be oxidized electrochemically to a silver(III) phthalocyanine that is also indefinitely stable. Further oxidation is possible to the silver(III) phthalocyanine cation radical, also showing substantial stability. Reduction to a silver(I) phthalocyanine leads to demetalation on the electrochemical time scale. In support of this electrochemical study, the electrochemistry of metal-free tetraneopentoxyphthalocyanine is also reported. Both silver(II) and metal-free tetraneopentoxyphthalocyanine are extensively aggregated in solution. The FTIR spectrum of the title complex is compared with the spectra of the corresponding cobalt(II), copper(II), and zinc species. The electronic spectra of the several silver species are reported. When diluted with metal-free tetraneopentoxyphthalocyanine, silver(II) tetraneopentoxyphthalocyanine yields a highly resolved electron spin resonance spectrum. Spin-Hamiltonian parameters are reported.

Introduction

The +2 and +3 oxidation states of silver can be stabilized by N_2-heterocyclic and tetraazamacrocyclic ligands and porphyrins,[1-6] but relatively little is known about these higher oxidation state silver species. While silver porphyrins have been studied in some

(1) Levason, W.; Spicer, M. D. *Coord. Chem. Rev.* **1987**, *76*, 45.
(2) Po, H. N. *Coord. Chem. Rev.* **1976**, *20*, 171.
(3) McMillan, J. A. *Chem. Rev.* **1962**, *62*, 65.
(4) (a) Kadish, K. M. *Prog. Inorg. Chem.* **1988**, 36, 365. (b) Kadish, K. M.; Lin, X. Q.; Ding, J. Q.; Wu, Y. T.; Araull, C. *Inorg. Chem.* **1986**, *25*, 3236.

0020-1669/90/1329-4090$02.50/0 © 1990 American Chemical Society

Table I. FTIR Data (cm^{-1})

$Ag^{II}TNPc$	734 s	824 m	1023 w	1057 s	1105 m	1124 s	1238 s		1283 m	1339 m	1609 s
$Cu^{II}TNPc$	747 s	822 m	1014 m	1061 s	1098 s	1120 m	1239 s	1272 w	1282 w	1344 m	1611 s
$Co^{II}TNPc$	751 s	821 m	1014 m	1065 s	1094 s	1128 s	1239 vs	1271 w	1283 w	1344 m	1611 s
$Zn^{II}TNPc$	744 s	823 m	1014 m	1057 s	1094 s	1122 s	1238 vs	1271 m	1283 m	1339 s	1610 vs

depth, silver phthalocyanine, although known for a long period[7] has not been seriously studied, probably because of its low solubility in organic solvents.

There is currently considerable interest in the development of phthalocyanine species for such high technology applications as electronic sensors, electrochromic displays, computer read–write disks, etc.[8,9] Silver phthalocyanine may have significant value in this context.

Recently, we have obtained the first highly soluble silver phthalocyanine species, silver(II) tetraneopentoxyphthalocyanine ($Ag^{II}TNPc$), and report here the characterization and properties of this species in several oxidation states. The species forms a Langmuir–Blodgett film whose properties will be described elsewhere.[10]

Experimental Section

Materials. Tetrabutylammonium hexafluorophosphate ($(TBA)PF_6$, Aldrich) was recrystallized from absolute ethanol and dried in a vacuum oven at 120 °C for 24 h. 1,2-Dichlorobenzene (DCB, Aldrich, Gold label) was used as supplied. Dichloroethane (DCE, Aldrich) was distilled over P_2O_5 before use.

(Tetraneopentoxyphthalocyanato)silver(II) ($Ag^{II}TNPc$). Metal-free tetraneopentoxyphthalocyanine (H_2TNPc)[11] (0.050 g, 5.8×10^{-5} mol) and silver nitrate (0.062 g, 3.6×10^{-4} mol) were heated in dimethylformamide (10 mL) at about 75 °C for about 6–7 h. Drops of the reaction mixture were removed from time to time to monitor the electronic absorption at 707 nm, due to H_2TNPc, relative to that at 685 nm, due to $Ag^{II}TNPc$. The reaction was stopped when the 707-nm peak had disappeared; the solution was stored overnight at room temperature. The resulting green precipitate was washed with water and acetone and recrystallized from toluene. Yield: 0.052 g, 93%. (Anal. CHN.)

Physical Measurements. Electronic spectra were recorded with a Hitachi Perkin-Elmer Model 340 microprocessor and Model 340 spectrometer or a Guided Wave Inc. Model 100-20 optical waveguide spectrum analyzer with a WW100 fiber optic probe. Electrochemical data were obtained with a Princeton Applied Research (PARC) Model 173 potentiostat or a PARC Model 174A polarographic analyzer coupled to a PARC Model 175 universal programmer. Cyclic voltammetry and differential-pulse voltammetry (DPV) were carried out under an atmosphere of argon, or nitrogen, by using a conventional three-electrode cell. The working electrode was described by the cross sectional area of a 27-gauge platinum wire (area 10^{-3} cm^2) and sealed in glass. A platinum wire also served as the counter electrode. The reference electrode was a small SCE separated from the working compartment by a glass frit or a silver-wire quasi-reference electrode. In the latter case, potentials were referenced internally to the ferrocenium/ferrocene (Fc^+/Fc) couple.

Controlled-potential electrolysis, coulometry, and spectroelectrochemical measurements were made by using a bulk electrolysis cell, consisting of a platinum-plate working electrode, platinum-flag counter electrode, and an SCE reference electrode. Counter and reference electrodes were separated from the working compartment by a glass frit and a salt bridge respectively. Spectra were recorded during bulk electrolysis by immersing the Guided Wave fiber optic probe in the solution, degassed with argon or nitrogen. Solutions for electrochemistry and spectroelectrochemistry contained 0.2–0.4 M $(TBA)PF_6$, as supporting electrolyte.

Electron spin resonance data were obtained by using a Varian E4 spectrometer calibrated with diphenylpicrylhydrazide. Isotropic spectra were measured in a chloroform solution at room temperature. To obtain anisotropic spectra at low temperature, a mixture of toluene and chloroform (1:1, v/v), was used, and a relatively large amount of metal-free tetraneopentoxyphthalocyanine (H_2TNPc) was added to the dilute (about 10^{-5} M) $Ag^{II}TNPc$ solution. A solution of pure $Ag^{II}TNPc$ does not yield a good spectrum at low temperature because of aggregation.

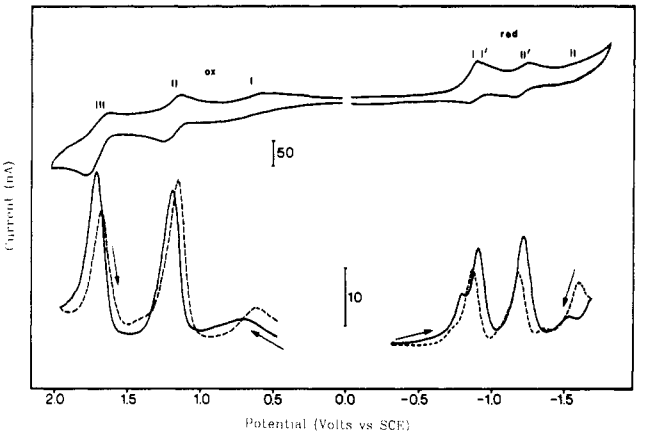

Figure 1. Cyclic and differential-pulse voltammograms for $Ag^{II}TNPc$ in DCB solution containing ca. 0.2 M $(TBA)PF_6$. Scan rates: 100 mV/s for CV and 2 mV/s for DPV. In the electrochemical studies, the concentration of AgTNPc is ca. 5×10^{-4} to 1×10^{-3} M.

Fourier Transform Infrared Spectra (FTIR). These were recorded as Nujol mulls using a Nicolet 20SX instrument. The principal absorption bands between 600 and 1800 cm^{-1} are given in Table I, with data for CuTNPc,[12] ZnTNPc,[13] and CoTNPc[14] for comparison.

Results and Discussion

Oxidation State. The ESR spectrum of $Ag^{II}TNPc$ is indicative of the d^9 Ag(II) ion. Furthermore, its FTIR spectrum is very similar to those of $Co^{II}TNPc$, $Cu^{II}TNPc$, and $Zn^{II}TNPc$ (see Table I). Note however that the FTIR spectra of these last three species are rather more similar to each other, in terms of relative band intensities and band shapes, than they are to that of $Ag^{II}TNPc$. Nevertheless, there is almost a 1:1 correlation with $Ag^{II}TNPc$ in terms of the number of bands and their positions.

Solubility and Stability in Solution. $Ag^{II}TNPc$ is highly soluble and stable in hydrocarbon and aromatic hydrocarbon solvents and their chlorinated derivatives and less soluble in nitrogen-containing solvents such as dimethylformamide and acetonitrile. It is insoluble in acetone and dimethyl sulfoxide. Indeed, coordinating solvents such as pyridine, rather than forming axially coordinated solvates as is common with chromium, iron, and cobalt phthalocyanines etc., lead to some demetalation as indicated by the electronic absorption spectra of the resulting solutions. AgTNPc is also demetalated by the addition of coordinating ligands such as imidazole, when such nitrogen ligands are added to otherwise stable solutions of AgTNPc, for example, in DCB. This lability of silver phthalocyanine has been attributed to the unfavorable relation between the radius of the silver(II) ion, relatively larger compared with first-series transition-metal ions, and the space available for it within the isoindole group.[15]

$Ag^{II}TNPc$ has a typical MPc(−2) electronic spectrum (see Figure 6) in very dilute (ca. 10^{-5} M) solution.[16] More concentrated solutions (e.g. $>10^{-4}$ M) show additional absorption at 620

(5) (a) Po, H. N.; Jones, S. E. *Inorg. Chim. Acta* **1981**, *48*, 37. (b) Jones, S. E.; Po, H. N. *Inorg. Chim. Acta* **1980**, *42*, 95. (c) Morano, D. J.; Po, H. N. *Inorg. Chim. Acta* **1978**, *31*, L421.
(6) Antipas, A.; Dolphin, D.; Gouterman, M.; Johnson, E. C. *J. Am. Chem. Soc.* **1978**, *100*, 7705.
(7) Barrett, P. A.; Frye, D. A.; Linstead, R. P. *J. Chem. Soc.* **1938**, 1157.
(8) Lever, A. B. P. *CHEMTECH* **1987**, *17*, 506.
(9) Snow, A. W.; Barger, W. R. In *Phthalocyanines, Properties and Applications*; Leznoff, C. C., Lever, A. B. P., Eds.; VCH: New York, 1989; p 341.
(10) Fu, Y. S.; Lever, A. B. P. Paper in preparation.
(11) Leznoff, C. C.; Marcuccio, S. M.; Greenberg, S.; Lever, A. B. P.; Tomer, K. B. *Can. J. Chem.* **1985**, *63*, 623.
(12) Kobayashi, N.; Lam, H.; Nevin, W. A.; Janda, P.; Leznoff, C. C. L.; Lever, A. B. P. *Inorg. Chem.*, in press.
(13) Manivannan, V.; Nevin, W. A.; Leznoff, C. C.; Lever, A. B. P. *J. Coord. Chem.* **1988**, *19*, 139.
(14) Nevin, W. A.; Hempstead, M. R.; Liu, W.; Leznoff, C. C.; Lever, A. B. P. *Inorg. Chem.* **1987**, *26*, 570.
(15) MacCragh, A.; Koski, W. S. *J. Am. Chem. Soc.* **1963**, *85*, 2375.
(16) Stillman, M. J.; Nyokong, T. In *Phthalocyanines, Properties and Applications*; Leznoff, C. C., Lever, A. B. P., Eds.; VCH: New York, 1989; p 133.

Table II. Electrochemical Data in Dichlorobenzene Solution[a]

	$E_{1/2}$, V (ΔE_p, mV)		
	$Ag^{II}TNPc$	H_2TNPc	assignments
oxidation			
III(ox)	1.72 irr		$[Ag^{III}Pc(0)]^{3+}/[Ag^{III}Pc(-1)]^{2+}$
II'(ox)		1.38 (120)	$[H_2TNPc(0)]^{2}/[H_2TNPc(-1)]^{+}$
II(ox)	1.19 (80)		$[Ag^{III}Pc(-1)]^{2+}/[Ag^{III}Pc(2-)]^{+}$
II'(ox)		0.9 irr	$[H_2TNPc(-1)]^{+}/H_2TNPc(-2)$
I(ox)	0.71 irr		$[Ag^{III}Pc(-2)]^{+}/Ag^{II}Pc(-2)$
reduction			
I(red)	−0.79[b]		$Ag^{II}TNPc(-2)/[Ag^{I}TNPc(-2)]^{-}$
I'(red)		−0.90 (70)	$H_2TNPc(-2)/[H_2TNPc(-3)]^{-}$
II'(red)		−1.20 (130)	$[H_2TNPc(-3)^{-}/[H_2TNPc(-4)]^{2-}$
II(red)	−1.47 (100)[c]		$[Ag^{I}TNPc(-2)]^{-}/[Ag^{I}TNPc(-3)]^{2-}$

[a] Potentials are reported with respect to SCE. $E_{1/2}$ values were measured by cyclic voltammetry at 20 mV s^{-1} [$E_{1/2} = (E_{pa} + E_{pc})/2$]. Peak to peak potentials are reported in parentheses. irr = irreversible. [b] Cathodic peak potential from differential-pulse voltammetry at 2 mV/s. [c] Peak to peak potential at 200 mV/s scan rate.

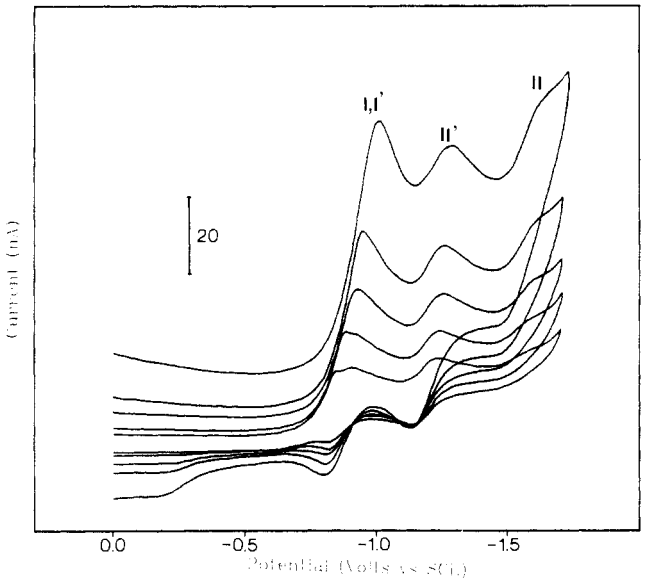

Figure 2. Variable scan rate cyclic voltammograms for $Ag^{II}TNPc$ in DCB/(TBA)PF_6 (reduction processes). Scan rates (inner to outer): 20, 50, 100, 200 and 500 mV/s.

nm indicative of aggregation common to phthalocyanine moieties.[14,17-19] Aggregation also occurs in very dilute solutions if they are cooled. Just above the freezing point of toluene (−95 °C), the 620-nm band, in a 1.5×10^{-5} M solution, has grown to some 83% of the intensity of the 685-nm band, and the whole Q-band region has broadened. As a result, the ESR spectrum of the Ag(II) species, clearly observed at room temperature (see below), is lost rather than intensified at lower temperature.

Electrochemistry. Figures 1 and 2 show cyclic and differential-pulse voltammograms for $Ag^{II}TNPc$ in DCB solution containing 0.2–0.4 M (TBA)PF_6 as supporting electrolyte.

$Ag^{II}TNPc(-2)$. Oxidation Processes. On the oxidation side, positive of 0 volts vs SCE, there are three redox couples. The first, I(ox), is broad, diffuse and contains several closely spaced waves. The second, II(ox), is a well-behaved reversible process, with equal cathodic and anodic currents and a square root dependence upon scan rate. The third, III(ox), is irreversible, showing an oxidation component but no return cathodic component (Table II).

On the basis of spectroelectrochemistry (described below), the ill-defined redox process I(ox) is assigned to the $[Ag^{III}TNPc(-2)]^{+}/Ag^{II}TNPc(-2)$ couple.[20] Controlled-potential oxidation over this wave generates a stable solution of $[Ag^{III}TNPc(-2)]^{+}$ (coulometry confirms this is a one-electron oxidation). The broad diffuse nature of couple I(ox) derives, at least in part, from aggregation phenomena in solution since the DPV peak becomes more narrow and better defined if the concentration is reduced. This is similar to the behavior reported by Kadish and co-workers[21] for zinc octacyanophthalocyanine, where both the monomeric and aggregated forms of the species oxidize at similar but not identical potentials.

Forward and reverse DPV scans show significantly shifted broad waves suggestive of a shift in the equilibrium mixture of monomeric and aggregated AgTNPc depending upon whether one is approaching from $Ag^{II}TNPc(-2)$ or $[Ag^{III}TnPc(-2)]^{+}$ (Figure 1). One must conclude that the kinetics of this equilibrium are sluggish with respect to the voltammetry time scale even on the very slow time scale of DPV.

Using a Nernstian plot of the spectroelectrochemical data over this first wave yields a half-wave potential for the Ag(III)/Ag(II) process of 0.71 V vs SCE. This is somewhat more positive than those for AgTPP and AgOEP, 0.54 and 0.44 V respectively,[4b] showing, as anticipated, the greater thermodynamic stability of silver(II) in a phthalocyanine environment relative to a porphyrin environment.

The reversible process, II(ox), is $[Ag^{III}TNPc(-1)]^{2+}/[Ag^{III}TNPc(-2)]^{+}$ with both the singly and doubly oxidized species being stable in DCB; it gives normal reversible forward and reverse DPV peaks, and is confirmed by coulometry to be a one-electron oxidation.

The irreversible couple III(ox) is not so securely assigned and it is not stable enough for spectroelectrochemical elucidation. It appears to have more current associated with it than does the previous couple, II(ox). It presumably involves the $[Ag^{III}TNPc(0)]^{3+}/[Ag^{III}TNPc(-1)]^{2+}$ couple: possibly the $[Ag^{III}TNPc(0)]^{3+}$ generated is then oxidizing solvent, or perhaps itself, resulting in some additional catalytic current.

$Ag^{II}TNPc(-2)$. Reduction Processes. In the electrochemistry of silver porphyrins, the Ag(II) central ion is reduced to Ag(I) prior to porphyrin ring reduction.[4b,6] However, demetalation is observed following the reduction of Ag(II) to Ag(I).[22,23] Well-defined CV waves for the $Ag^{II}TPP/[Ag^{I}TPP]^{-}$ reduction were observed with $E_{1/2}$ at −1.01 V vs SCE in dichloromethane. In the same solvent, H_2TPP is reduced at −1.21 V vs SCE. The Ag(II)/Ag(I) reduction wave is rather broad, and the current ratio I_{pa}/I_{pc} is less than unity at low sweep rates and approaches unity at higher sweep rates. This is consistent with reduction of $Ag^{II}TPP$ to $[Ag^{I}TPP]^{-}$ followed by demetalation at a rate comparable to the cyclic voltammetric time scale. Controlled-potential electrolysis just negative of the Ag(II)/Ag(I) wave leads to the unmetalated

(17) Nevin, W. A.; Liu, W.; Greenberg, S.; Hempstead, M. R.; Marcuccio, S. M.; Melnik, M.; Leznoff, C. C.; Lever, A. B. P. *Inorg. Chem.* **1987**, *26*, 891.
(18) Lever, A. B. P. *Adv. Inorg. Chem. Radiochem.* **1967**, *7*, 27.
(19) Nevin, W. A.; Liu, W.; Lever, A. B. P. *Can. J. Chem.* **1986**, *65*, 855.
(20) Myers, J. F.; Rayner Canham, G. W.; Lever, A. B. P. *Inorg. Chem.* **1975**, *14*, 461. This paper defines the nomenclature for phthalocyanine redox species.
(21) Giraudeau, A.; Louati, A.; Gross, M.; Andre, J. J.; Simon, J.; Su, C. H.; Kadish, K. M. *J. Am. Chem. Soc.* **1983**, *105*, 2917.
(22) Giraudeau, A.; Louati, A.; Callot, H. J.; Gross, M. *Inorg. Chem.* **1981**, *20*, 769.
(23) Kumar, A.; Neta, P. *J. Phys. Chem.* **1981**, *85*, 2830.

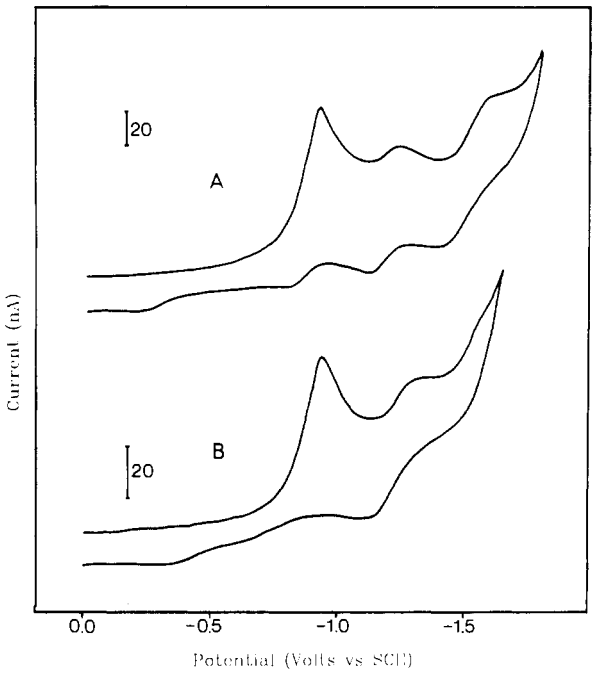

Figure 3. (A) Cyclic voltammogram for reduction of $Ag^{II}TNPc$ at −15 °C in DCB/(TBA)PF_6. Scan rate: 100 mV/s. (B) Cyclic voltammogram for reduction of $Ag^{II}TNPc$ at room temperature in DCE/(TBA)-PF_6. Scan rate: 100 mV/s.

free base. The lability of silver porphyrins was attributed to the fact that the diameter of Ag(I) ion is 1.26 Å but that of Ag(II) is only 0.89 Å. Expulsion of Ag(I) from the porphyrin core evidently takes place.

$Ag^{II}TNPc$ has very similar electrochemical behavior. There are four reduction processes between 0 and −1.5 V vs SCE, namely I(red), I′(red), II′(red), and II(red) (Figure 1), with I(red) and I′(red) overlapping, in the cyclic voltammogram. Wave II′(red) is a well-behaved reversible couple with equal cathodic and anodic currents and a square root dependence upon scan rate. Controlled-potential reduction just negative of the first composite wave (I(red)) leads only to the reduced metal free $[H_2TNPc(-3)]^-$ anion radical.

The composite nature of this first reduction is more clearly demonstrated in the DPV voltammogram, which shows two peaks separated by ca. 95 mV. In the CV experiment, with increasing scan rate, peak I(red) shifts more negatively, moving underneath peak I′(red), which only shifts slightly negative under these conditions (Figure 2). Couple II(red) becomes more obvious at higher scan rates, with intensity growing at the expense of couple II′(red). It is largely absent from the very slow scans, especially for example the DPV scans, which are carried out at 2 mV/s. Normal forward (negative going from 0 V) and reverse (positive going from negative potentials toward 0 V) DPV scans are observed for couples I′(red) and II′(red), but I(red) appears only in the forward DPV scan (Figure 1). In the cooled solution, (Figure 3A), wave I(red) becomes highly irreversible, while wave II′(red) becomes relatively less intense and wave II(red) becomes relatively more intense.

These data lead to the following redox assignments (Table II):

$$\text{I(red)}\quad Ag^{II}TNPc(-2)/[Ag^{I}TNPc(-2)]^- \quad E_{irr}$$

followed by

$$[Ag^{I}TNPc(-2)]^- + 2H^+ \rightarrow H_2TNPc(-2) + Ag(I) \quad C_{irr}\ \text{(slow)}$$

followed by

$$\text{I′(red)}\quad H_2TNPc(-2)/[H_2TNPc(-3)]^- \quad E_{rev}$$

$$\text{II′(red)}\quad [H_2TNPc(-3)]^-/[H_2TNPc(-4)]^{2-} \quad E_{rev}$$

$$\text{II(red)}\quad [Ag^{I}TNPc(-2)]^-/[Ag^{I}TNPc(-3)]^- \quad E_{rev}$$

The voltammetry of H_2TNPc (described briefly below) shows two reduction processes at the same potentials as I′(red) and II′(red), and indeed addition of some H_2TNPc to a $Ag^{II}TNPc$ solution results in a comparative increase in the currents for I′(red) and II′(red). Furthermore, the voltammogram for H_2TNPc does not show a wave in the position for II(red), confirming that it is a silver-based couple.

The demetalation of $[Ag^{I}Pc]^-$ likely proceeds through a hydrolysis step involving trace moisture in the solvent. However, intensive drying of the solvent with molecular sieves did not materially alter the electrochemistry described here. At high scan speeds, there is less time for demetalation of $Ag^{I}TNPc(-2)$, and therefore II′(red) is suppressed and the second silver phthalocyanine reduction, II(red), is enhanced. Similarly at low temperatures, demetalation is suppressed.

Redox process I(red) shifts to more negative potentials with increasing scan rate because it is an $E_{irr}C_{irr}$ process; because of the overlapping nature of the band, detailed analysis of this shift with scan rate is deferred. The electron-transfer irreversibility is indicated by the fact that even at low temperatures little or no return current can be assigned to I(red) (Figure 3A). This is also clearly seen in Figure 3B, which shows the behavior in dichloroethane.

The absence of a reverse DPV peak for I(red) is a consequence of the buildup of H_2TNPc and a depletion of AgTNPc in the vicinity of the electrode when scanned from very negative potentials.

More detailed consideration of the relative currents evident in the low-temperature voltammogram (Figure 3A) suggests that there may be an intermediate step between the reduction of $Ag^{II}TNPc$ and the hydrolysis of $[Ag^{I}TNPc]^-$ since less metal-free H_2TNPc appears present than a rough estimate of the amount of AgTNPc that has hydrolyzed.[24] One might have also expected that the Ag(II)/Ag(I) electron-transfer step would have shown reversibility at low temperature when the hydrolysis was partially suppressed since metal couples within MPc units are usually reversible in the absence of a following reaction. Possibly the intermediate causing irreversibility is a sitting-atop $Ag^{I}TNPc$ species, the large metal ion having popped out of the plane of the macrocycle.

There are some alternative assignments for the redox electrochemistry that must be considered but which may in fact be rejected:

	I(red)	II(red)
(i)	$Ag^{II}TNPc(-2)/[Ag^{II}TNPc(-3)]^-$	$[Ag^{II}TNPc(-3)]^-/[Ag^{II}TNPc(-4)]^{2-}$
(ii)	$Ag^{II}TNPc(-2)/[Ag^{II}TNPc(-3)]^-$	$[Ag^{II}TNPc(-3)]^-/[Ag^{I}TNPc(-3)]^{2-}$

The couples in assignment i, by analogy with the copper TNPc species[12] and species such as H_2TNPc reported here, would be separated by about 0.3–0.4 V and not, as observed here, by ca. 0.65 V. Assignment ii is also logically unacceptable for the same reason; i.e., $[Ag^{II}TNPc(-3)]^-$ would be reduced to $[Ag^{II}TNPc(-4)]^{2-}$, some 0.3–0.4 V negative of I(red), before reduction to $[Ag^{I}TNPc(-3)]^{2-}$ could take place.

The assignments chosen here (Table II) are also supported by the observation that the reduction process $[Co^{I}TNPc(-2)]^-/[Co^{I}TNPc(-3)]^{2-}$ occurs, in DCB, at a potential very close to that of process II(red).[12]

$H_2TNPc(-2)$. The voltammogram for this species in DCB is shown in Figure 4, with data collected in Table II. This species was explored briefly to obtain data with which to compare the AgTNPc behaviors described above. There are two clearly defined reversible reduction processes, I′(red) and II′(red), uniquely assignable to $H_2TNPc(-2)/[H_2TNPc(-3)]^-$ and $[H_2TNPc(-3)]^-/[H_2TNPc(-4)]^{2-}$, respectively.

(24) We are grateful to a reviewer for bringing this to our attention.

Table III. Electronic Absorption Maxima[a]

species	λ_{max}, nm ($10^{-4}\epsilon$, M^{-1} cm^{-1})					
$Ag^{II}TNPc(-2)$	356 (1.33)	386 (1.07)		618 (2.12)	685 (7.61)	
$[Ag^{III}TNPc(-2)]^{+}$ [b]	361 (0.80)	424 (1.77)		647 (2.02)	722 (6.78)	
$[Ag^{III}TNPc(-1)]^{2+}$ [b]		439 (1.92)	574 (1.14)	649	721 (0.95)	854 (1.06)

[a] DCB solution. [b] Solutions contain about 0.2 M $(TBA)PF_6$.

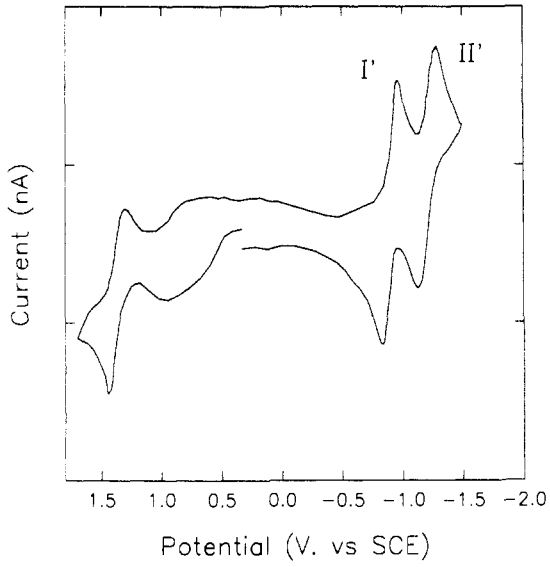

Figure 4. Cyclic voltammogram of H_2TNPc in DCB/$(TBA)PF_6$. Scan rate: 100 mV/s.

Positive of 0 V are seen two redox processes curiously similar to the AgTNPc data described here. There is a broad redox wave positive of 0 V, I'(ox), which must arise from oxidation of both mononuclear and aggregated $H_2TNPc(-2)$ to $[H_2TNPc(-1)]^{+}$. The more positive and reversible redox process II'(ox) is then assigned to $[H_2TNPc(0)]^{2+}/[H_2TNPc(-1)]^{+}$.

Spectroelectrochemistry of AgTNPc Species. Stepwise controlled-potential oxidation from 0.55 to 0.9 V (vs SCE) of a solution of $Ag^{II}TNPc$ in DCB with $(TBA)PF_6$ as supporting electrolyte results in the spectroscopic changes shown in Figure 5a, and a change in solution color from blue to greenish yellow. Isosbestic points are observed at 395, 557, and 703 nm. The final spectrum is consistent with that of a MPc(−2) species and not an oxidized MPc(−1) species,[14,20] and therefore oxidation to $[Ag^{III}TNPc(-2)]^{+}$ has occurred. Both the Q-band and the Soret band shift to longer wavelength by about 40 nm in the Ag(III) species compared with the Ag(II) species.

Figure 5b shows the spectrum development in the stepwise controlled-potential electrolysis in the range 1.10–1.40 V, of the $[Ag^{III}TNPc(-2)]^{+}$ generated by bulk electrolysis at 0.95 V. Isosbestic points are found at 612 and 752 nm. The solution color changes from greenish yellow to dark gray. During this oxidation, the Q-band loses intensity and broad low-intensity bands appear in the 500–600- and 800–900-nm regions. These are characteristic of the formation of radical Pc(−1) species,[13,14,17,20,25] specifically $[Ag^{III}TNPc(-1)]^{2+}$.

The spectroscopic changes for both oxidation steps (Figure 5a,b) were reversible, and the original $[Ag^{III}TNPc]^{+}$ and $Ag^{II}TNPc$ spectra were generated by reverse stepwise controlled-potential reductions from 1.35 to 1.10 V and from 0.9 to 0.5 V, respectively. Thus these data confirm the electrochemical assignments indicated above (Table II).

Plots of log $[(A_0 - A)/(A - A_\infty)]$ vs potential for the two oxidation steps and their rereductions gave the expected linear plots. Zero intercepts give an apparent $E_{1/2}$ of 0.71 V for the $[Ag^{III}TNPc(-2)]^{+}/Ag^{II}TNPc(-2)$ couple (data from Figure 5a

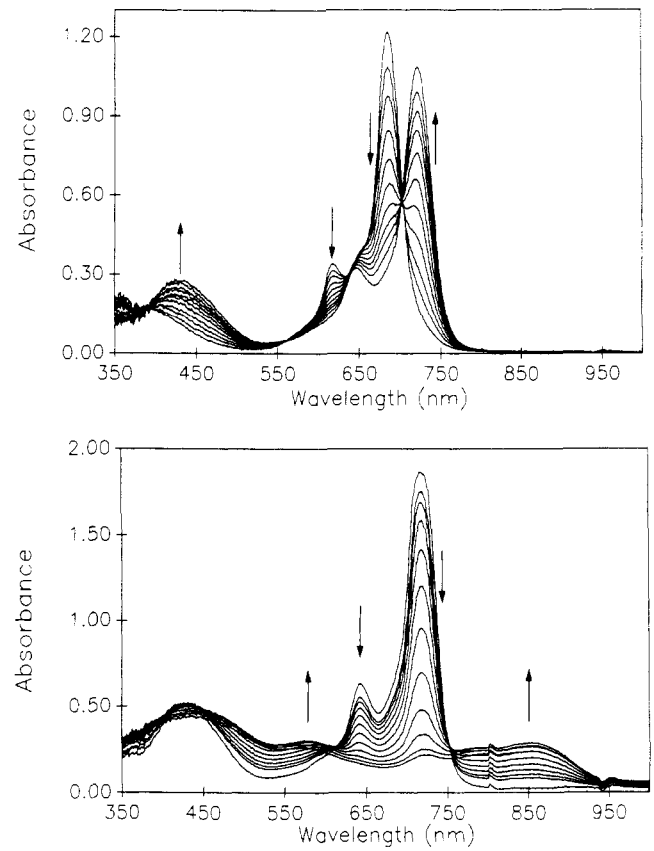

Figure 5. Stepwise controlled-potential spectroelectrochemistry: (a) $Ag^{II}TNPc$ in DCB solution showing the development of $[Ag^{III}Pc(-2)]^{+}$ as potential is stepped through the first oxidation wave from 0.55 to 0.9 V vs SCE; (b) Electrochemically generated $[Ag^{III}Pc(-2)]^{+}$ in DCB showing the development of the π cation radical $[Ag^{III}Pc(-1)]^{2+}$ as the potential is stepped through the second oxidation wave from 1.10 to 1.40 V vs SCE. The solutions contain ca. 0.2 M $(TBA)PF_6$. The absorbance value for the main peak near 722 nm, ca. 2.00, is rather high, and the top of the band may be clipped slightly. The data in Figure 6 are more accurate. Base-line "glitches" near 803 and 941 nm are machine artifacts and should be ignored. The concentration of $Ag^{II}TNPc$ is ca. 3×10^{-5} M.

at 685 nm) and 1.25 V for the $[Ag^{III}TNPc(-1)]^{2+}/[Ag^{III}TNPc(-2)]^{+}$ couple (data from Figure 5b at 722 nm). The latter line has a slope of 77 mV (average of forward and reverse experiments) close to the anticipated 59 mV for a one-electron redox process. The former line has an average slope of about 110 mV, larger than expected; the reason for this is not apparent. The spectroelectrochemical data were obtained at a concentration some 10–20 times more dilute than the electrochemical data, in a regime where aggregation, though present, is very much less important.

Figure 6 shows the electronic absorption spectra of $Ag^{II}TNPc$ and the electrochemically generated $[Ag^{III}TNPc(-2)]^{+}$ and $[Ag^{III}TNPc(-1)]^{2+}$ species. Absorption maxima and molar absorptivity data are given in Table III.

Electron Spin Resonance. The Ag(II) species has a d^9 configuration with one unpaired electron. Extensive ESR studies have been carried out on silver(II) *N*-heterocyclic complexes[2] and silver(II) porphyrins[26,27] and also the isoelectronic copper(II)

(25) Leznoff, C. C.; Lam, H.; Marcuccio, S. M.; Nevin, W. A.; Janda, P.; Kobayashi, N.; Lever, A. B. P. *J. Chem. Soc., Chem. Commun.* **1987**, 699.

(26) (a) MacCragh, A.; Storm, C. B.; Koski, W. S. *J. Am. Chem. Soc.* **1965**, *87*, 1470. (b) Kneubuhl, F. K.; Koski, W. S.; Caughey, W. S. *J. Am. Chem. Soc.* **1961**, *83*, 1607.

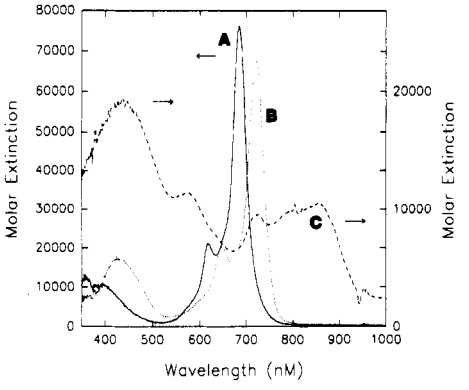

Figure 6. Electronic absorption spectra: (A) (--) $Ag^{II}TNPc$ in DCB; (B) (···) electrochemically generated $[Ag^{III}TNPc(-2)]^{+}$; (C) (--) $[Ag^{III}TNPc(-1)]^{2+}$ in DCB solution with ca. 0.2 M $(TBA)PF_6$. Note that the first two spectra are plotted versus the left-hand y axis, while the third spectrum is expanded through use of the right-hand y axis. Base-line "glitches" near 373, 803, and 941 nm are machine artifacts and should be ignored.

Table IV. Spin Hamiltonian Parameters[a]

		hyperfine coupling to Ag		superhyperfine coupling to N	
g	g value	param	value, G	param	value, G
g_{iso}	2.049	a	52	b	23.6
$g_{\parallel}$	2.087	A	40	C	20
$g_{\perp}$	2.030	B	58	D	25.4

[a] a and b are the isotropic hyperfine coupling constants to silver and nitrogen, respectively. A and B are the anisotropic hyperfine coupling constants parallel and perpendicular to silver, respectively. C and D are the anisotropic hyperfine coupling constants parallel and perpendicular to nitrogen, respectively.

phthalocyanines.[28] Few ESR data are available for silver phthalocyanines. MacCragh and Koski[15] reported some ESR parameters for AgPc in 1963 within work mainly devoted to porphyrin species. They experienced difficulties because of the low solubility and lability of the species.

The ESR spectra of $Ag^{II}TNPc$ in chloroform at room temperature and diluted with H_2TNPc, in chloroform/toluene glass at 98 K are shown in parts a and b of Figure 7. Dilution with H_2TNPc is necessary to reduce the effects of relaxation caused by aggregation when solutions of $Ag^{II}TNPc$ are cooled. Evidently H_2TNPc can replace $Ag^{II}TNPc$ in aggregated species, yielding $Ag^{II}TNPc{\cdot}H_2TNPc$ aggregates, which generate fine quality ESR spectra.

Silver has two isotopes, both of nuclear spin of 0.5 and of approximately equal abundance. There are four equivalent nitrogen atoms, each with nuclear spin 1.0. Thus, assuming equal coupling to the two silver isotopes, there could be 18 lines in the spectra of each of the parallel and perpendicular orientations. The isotropic spectrum shows 11 roughly equally spaced lines (Figure 7a) which arise if the silver isotropic hyperfine coupling constant

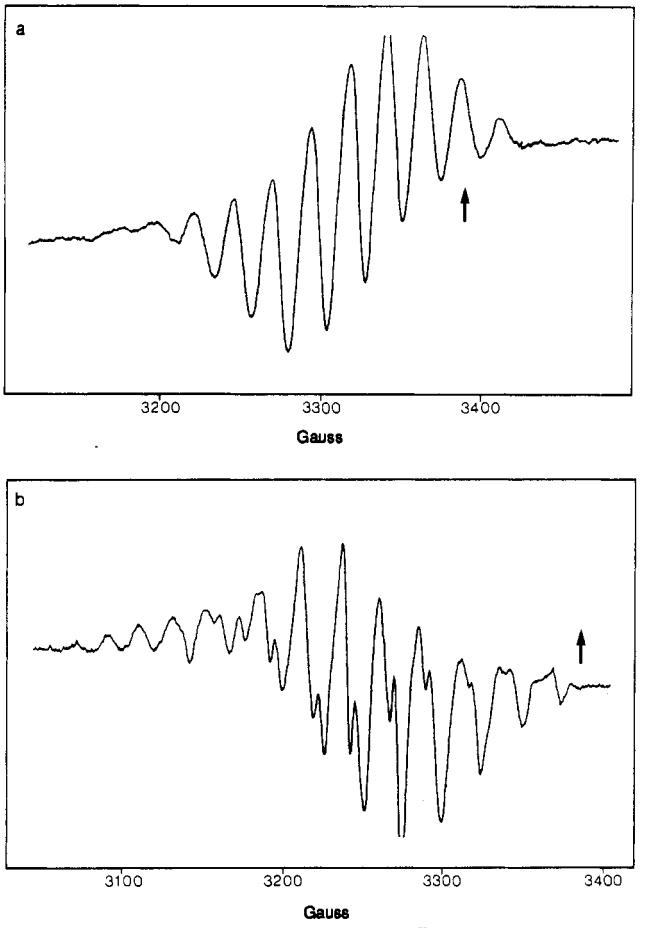

Figure 7. Electron spin resonance spectra of $Ag^{II}TNPc$ (a) in chloroform solution at room temperature and (b) in a mixed chloroform/toluene (1:1, v/v) solvent, at 98K, containing ca. 10^{-3} M H_2TNPc to reduce the self-aggregation of the silver species. The arrow indicates the free spin g value.

is (approximately) twice that of the nitrogen isotropic hyperfine coupling constant. The frozen-solute ESR spectrum (Figure 7b) is resolved into at least 24 lines. From the analysis used by Koski et al.[15,26] in their studies on copper and silver porphyrins, computer simulation of the anisotropic spectrum yielded the spin-Hamiltonian parameters given in Table IV. Though the quality of the data reported here exceeds that of data published previously,[15] the actual parameters derived here for $Ag^{II}TNPc/H_2TNPc$, in DCB, do not differ significantly from those of $Ag^{II}Pc$ in 1-chloronaphthalene.

Conclusion. Silver(II) tetraneopentoxyphthalocyanine is a well-characterized silver phthalocyanine whose solubility in organic solvents should make it valuable for future film studies. It is especially pertinent that both the one- and two-electron oxidation products are also stable. Future studies will explore this oxidation chemistry in film phase.

Acknowledgment. We are indebted to the Natural Sciences and Engineering Research Council (Ottawa) and the Office of Naval Research (Washington, DC) for financial assistance.

(27) Brown, T. G.; Hoffman, B. M. *Mol. Phys.* **1980**, *39*, 103.
(28) Roberts, E. M.; Koski, W. S. *J. Am. Chem. Soc.* **1961**, *83*, 1865.